



Comparative Study of the Effects of Growth Temperature, Annealing Temperature, and Calcination Temperature on the Size and Bandgap of ZnO Nanoparticles

Zuhoor Elahi^{1,2,*} and Wafa Gull²

¹Department of Physics, University of Karachi, Pakistan

²Department of Physics and Astronomy, University of Southern Mississippi, USA

*Corresponding author: Zuhoor Elahi, Department of Physics, University of Karachi, Pakistan

Received date: 01 October 2023; Accepted date: 11 October 2023; Published date: 18 October 2023

Citation: Elahi Z, Gull W (2023). Comparative Study of the Effects of Growth Temperature, Annealing Temperature, and Calcination Temperature on the Size and Bandgap of ZnO Nanoparticles. *SunText Rev Mat Sci* 4(1): 123.

DOI: <https://doi.org/10.51737/2766-5100.2023.023>

Copyright: © 2023 Elahi Z, et al. This is an open-access article distributed under the terms of the Creative Commons Attribution License, which permits unrestricted use, distribution, and reproduction in any medium, provided the original author and source are credited.

Abstract

The Zinc Oxide (ZnO) nanoparticles were successfully synthesized by solgel method using Zinc nitrate hexahydrate and sodium hydroxide. Obtained nanoparticles were successfully analyzed for structural, optical, morphological, and compositional studies using XRD, UV-VIS, SEM, and EDX analysis techniques respectively. The structure of ZnO was found to be hexagonal wurtzite. The crystallite sizes of the three sets of nanoparticles samples were successfully calculated using the Scherrer formula and found the dependence on the growth temperature, annealing temperature, and calcination temperature. The bandgaps of the particles were also determined from the UV-VIS spectra. UV-VIS spectroscopy reveals that UV absorption characteristics can be tuned by varying the annealing and calcination temperatures. The SEM images show that most of the samples consist of spherical nanoparticles. UV-Visible spectroscopy reveals that UV absorption characteristics can be tuned by varying the calcination temperature.

Keywords: Nanoparticles; Crystallite size; Bandgap; Annealing; Calcination

Introduction

Band gap engineering is becoming an effective tool for tailoring the properties of materials [1]. At nanoscale quantum confinement effects become dominant which derives the material to show different properties as they show in bulk [2]. There are a lot of methods to synthesize the desired nanoparticles (ZnO), but we are choosing one of the low-cost methods, the Sol-gel method. Several studies have shown that ZnO is proven to be non-toxic for human cells and toxic for bacteria. This property made it biocompatible [3]. Semiconductor NPs possess wide bandgaps and therefore showed significant alteration in their properties with bandgap tuning. Therefore, they are very important materials in photocatalysis, photo-optics and electronic devices [4]. As an example, variety of semiconductor nanoparticles are found exceptionally efficient in water splitting applications, due to their suitable bandgap and bandgap positions [5]. The various properties of nanoparticles such as physical, optical, etc. can be

tailored by varying temperature at the time of their growth, annealing, and calcination etc. Annealing help to improving the crystallinity of ZnO nanoparticles [6,7]. It can take place in air or in neutral or reducing atmospheres, but usually is done in air. A terminology used both in metallurgy and in the case of thin films, referring to a heat treatment process that helps to reduce residual stress and hence decrease defects in any structure [8]. The idea is to give the atoms some mobility through thermal energy, such that they can diffuse to the lower energy (more stable) position. Calcination is used to increase crystallinity of material [9]. In case of any impurities present on the surface is also removed and calcination temperature utilized to prepared material converted one phase to other [10]. Calcination temperature generally favors crystal growth [11]. In this paper we discussed the effects of temperature at the time of growth, annealing, and calcination on crystallite size and bandgap of the synthesized ZnO nanoparticles.

The obtained results are then compared to see the effects of different synthesis conditions.

Experimental Setup

Zinc oxide nanoparticles were synthesized by wet chemical method using zinc nitrate and sodium hydroxide precursors. A 0.5M aqueous ethanol solution of zinc nitrate hexahydrate ($\text{Zn}(\text{NO}_3)_2 \cdot 6\text{H}_2\text{O}$), and a 0.9M aqueous ethanol solution of sodium hydroxide (NaOH) were kept under constant stirring using magnetic stirrer to completely dissolve the zinc nitrate for one hour. The 0.9M NaOH aqueous solution was added under high-speed constant stirring, drop by drop (slowly for one hour) touching the walls of the vessel. The stirring continued for two more hours, and the beaker was sealed at this condition. The solution was allowed to settle for overnight and further, the supernatant solution was separated carefully. The remaining solution was centrifuged for 10 min, and the precipitates were removed. The precipitated ZnO NPs were cleaned three times with deionized water and ethanol to remove the by products, and then dried in furnace at about 60°C for 48 hours (2 days). The first set of five samples are grown at different temperatures, that is at RT (room temperature), 30°C, 40°C, 50°C, and 60°C. The second set of five dried samples (grown at room temperature) are annealed at 200°C, 300°C, 400°C, 500°C, and 600°C in a furnace. The third set of samples was calcined at 450°C, 500°C, 550°C, 600°C, and 650°C. The process is shown schematically in (Figure 1).

Observations

Structural analysis

The XRD patterns of the samples grown, annealed, and calcined at different temperatures are shown in (Figures 2-4), respectively which show that the ZnO nanoparticles have hexagonal wurtzite structure. The crystallite sizes and lattice constants are found by applying Gaussian fit in the Origin lab (Origin 2023b), and, using the Scherrer formula. The calculated values are plotted against the growth, annealing, and calcination temperatures in (Figures 5-7) respectively, and listed in (Tables 1-3) respectively. Figure 5 shows that the crystallite size increases as we increase the growth temperature. The value of the lattice constant has an average value of 3.2542Å for the first four data points, and decreased in the fifth point, but that change is at the third decimal place which is not a significant change. In the case of annealing temperature, Figure 6 shows that the crystallite is again increased with increasing temperatures, as was the case of increasing growth temperatures, while the lattice constant oscillates between 3.2505Å and 3.2661Å. In contrast to previous cases, Figure 7 shows that the crystallite size decreases with the increase in calcination temperature. The crystallite sizes are observed to be

decreased from 26.84nm to 25.25nm for the temperatures range of 450°C to 650°C. The lattice constant also follows a path like that of the crystallite size having values ranging 20 from 3.2571Å to 3.2529Å.

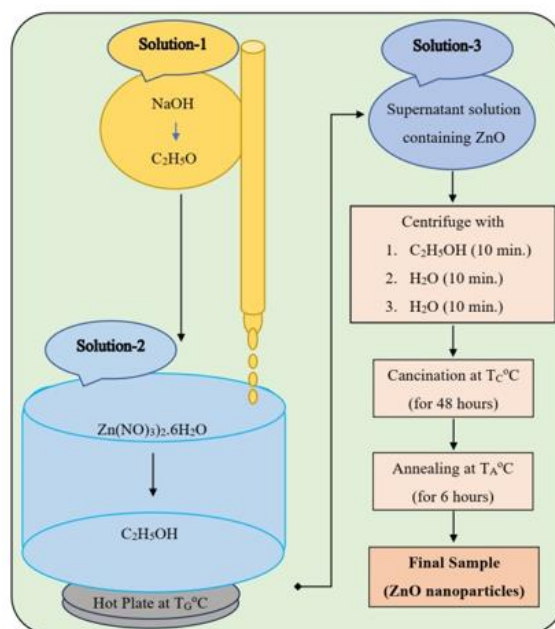


Figure 1: Experimental setup.

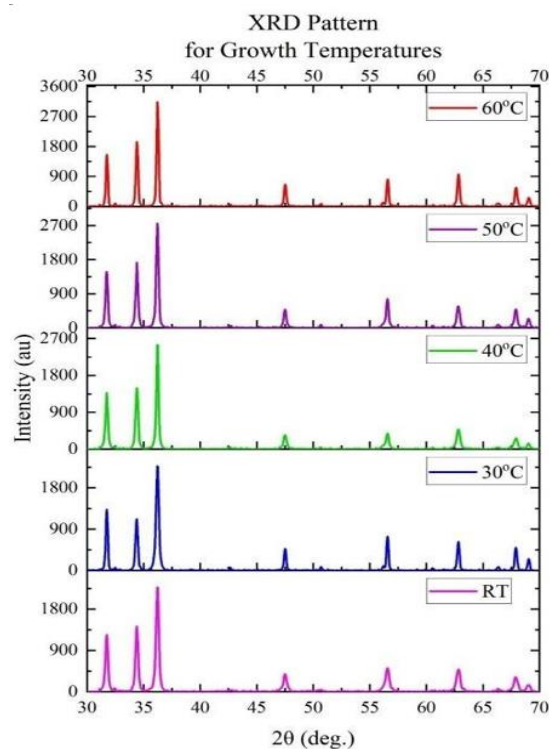


Figure 2: XRD patterns of the samples grown at different temperatures.

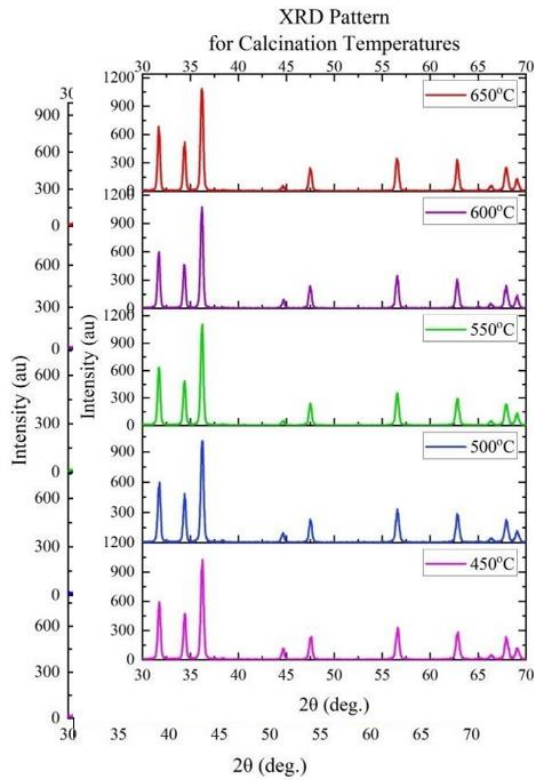


Figure 3: XRD patterns of the samples annealed at different temperatures.

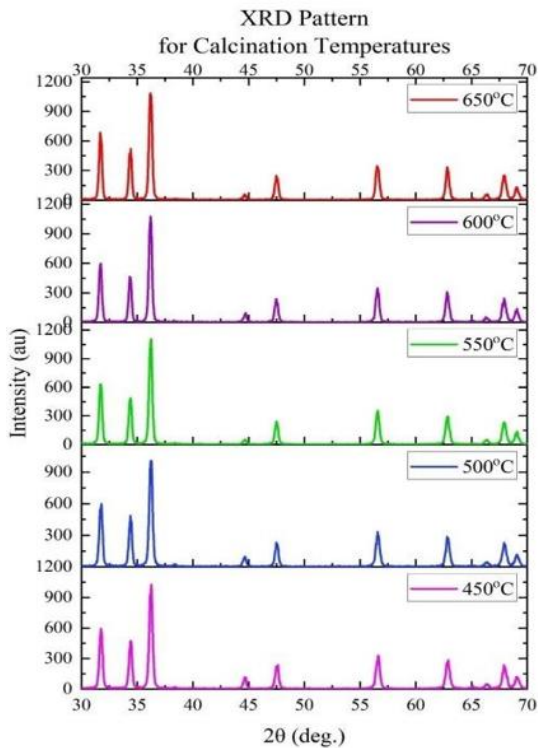


Figure 4: XRD patterns of the samples calcined at different temperatures.

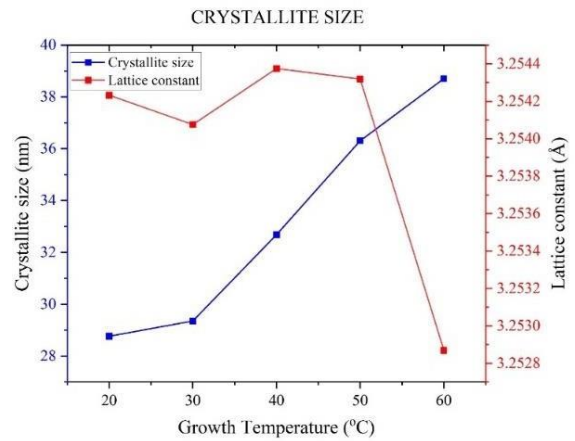


Figure 5: Crystallite size (blue) and lattice constant (red) for the samples grown at different temperatures.

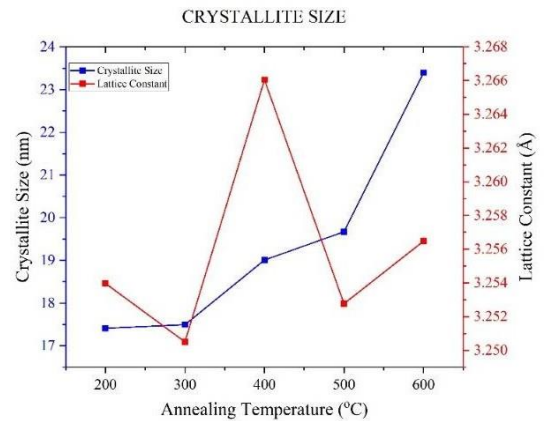


Figure 6: Crystallite size (blue) and lattice constant (red) and lattice constant for the samples annealed at different temperatures.

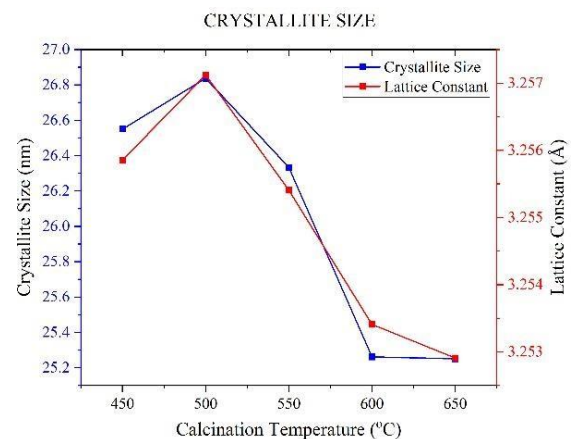


Figure 7: Crystallite size (blue) and lattice constant (red) and lattice constant for the samples calcined at different temperatures.

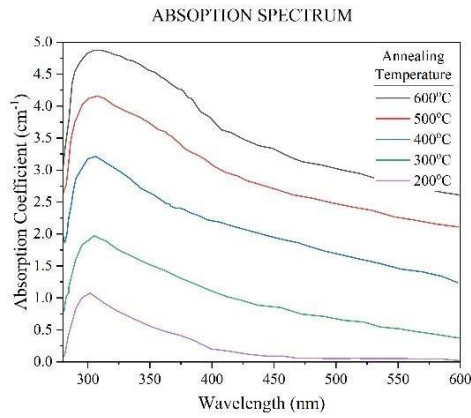


Figure 8: Absorption spectrum for the samples annealed at different temperatures.

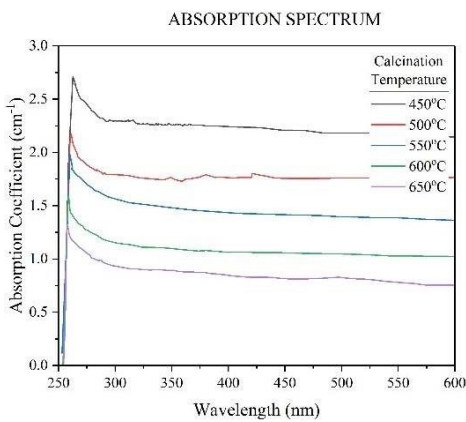


Figure 9: Absorption spectrum for the samples calcined at different temperatures.

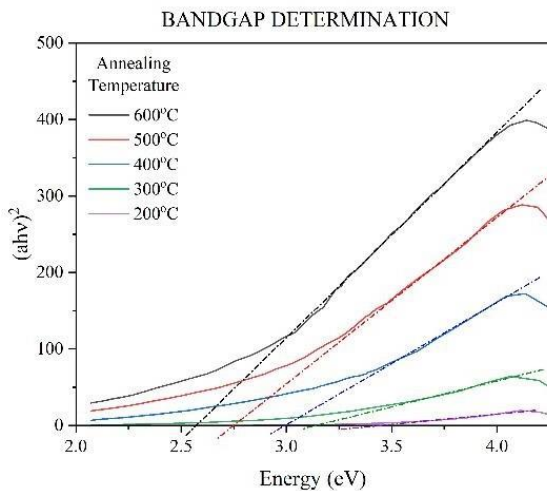


Figure 10: Optical absorption against photon energy is plotted to find the bandgap by drawing the slopes (broken lines) for the samples annealed at different temperatures.

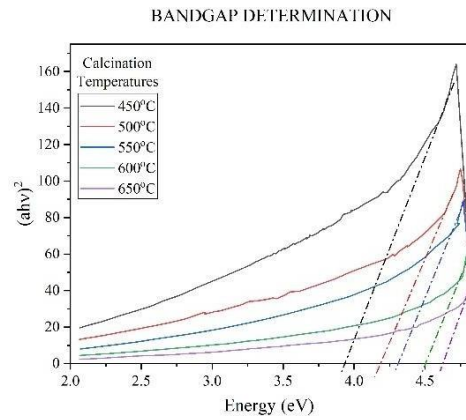


Figure 11: Optical absorption against photon energy is plotted to find the bandgap by drawing the slopes (broken lines) for the samples calcined at different temperatures.

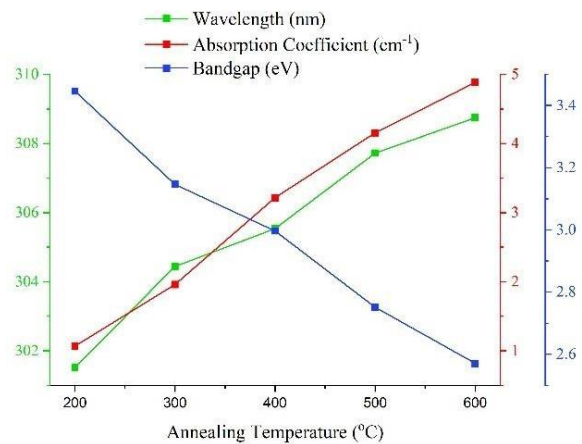


Figure 12: Peak wavelengths, absorption coefficients, and the bandgap energy as functions of annealing temperatures.

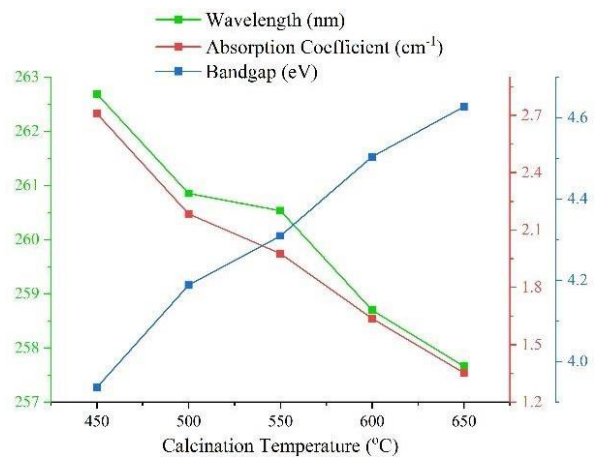


Figure 13: Peak wavelengths, absorption coefficients, and the bandgap energy as functions of calcination temperatures.

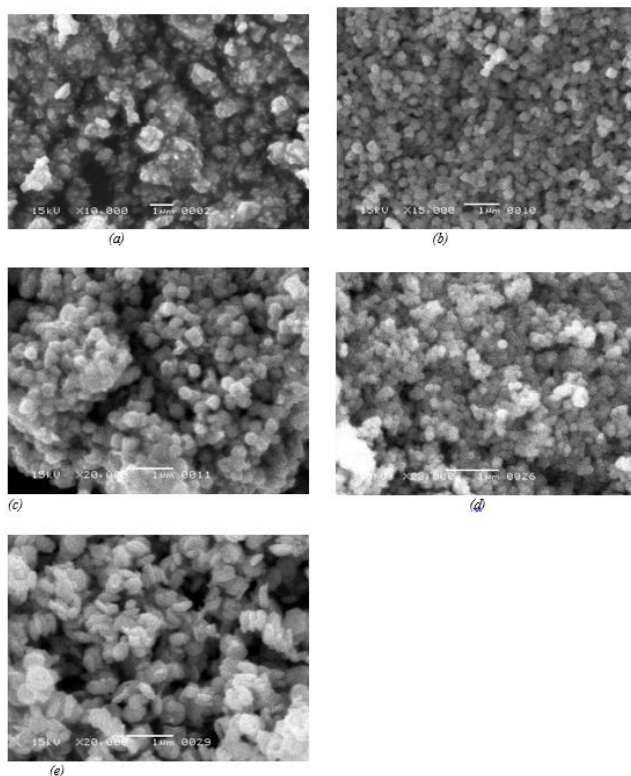


Figure 14: SEM images of samples for growth temp. (a) Room Temperature, (b) 30°C, (c) 40°C, (d) 50°C, and (e) 60°C

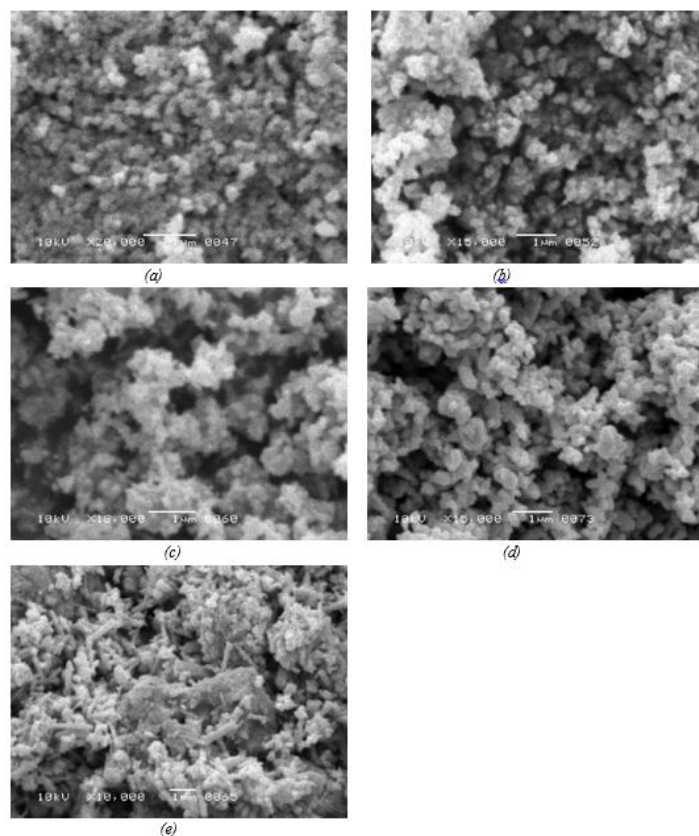


Figure 16: SEM images of samples for Calcination temperatures (a) 450°C, (b) 500°C, (c) 550°C, (d) 600°C, and (e) 650°C

Optical Analysis

Absorption spectrum

The effects of annealing and calcination temperatures on the optical properties of the ZnO nanoparticles were studied by UV-VIS absorption spectroscopy. Graph of Figure 8 shows the optical absorption spectra of ZnO nanoparticles annealed at different temperatures. The absorption peaks are observed to increase from 301.52 nm to 308.75 nm for the annealing temperatures of 200°C to 600°C respectively. A slight redshift in absorption peak for the samples annealed at different temperatures was noticed. It is known that the ZnO particles which have absorption at higher wavelength in the UV-visible spectrum have higher particles size. With increasing temperature, the particle size increases, and the peak absorbance wavelength becomes redshifted due to decreasing quantum confinement. The graph of Figure 9 shows the optical absorption spectra of ZnO nanoparticles calcined at different temperatures. In contrast to the previous case a blueshift was observed in the case of increasing calcination temperatures.

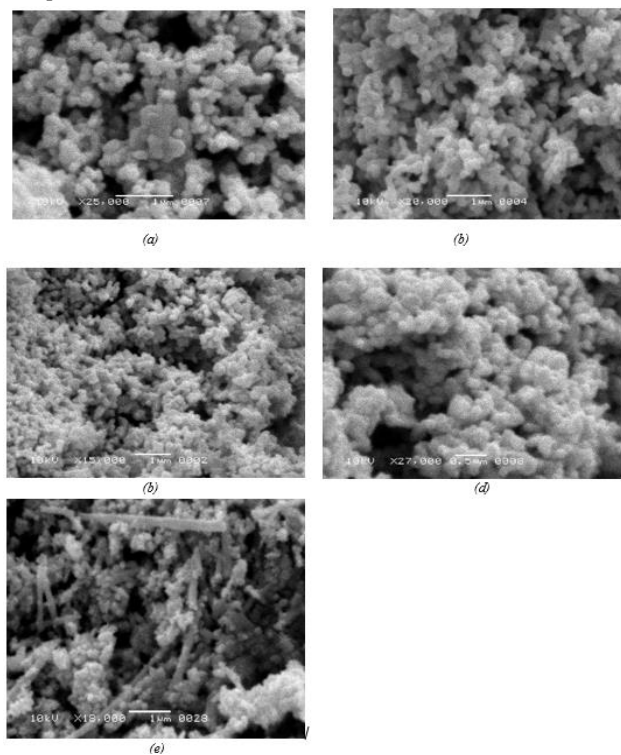


Figure 15: SEM images of samples for Annealing temperatures (a) 200°C, (b) 300°C, (c) 400°C, (d) 500°C, and (e) 600°C

Bandgap

The optical bandgaps of the prepared samples are estimated by plotting $(\alpha h\nu)^2$ against $h\nu$ and using the Tauc relation given below, and extrapolation procedure as shown in Figure 10 and Figure 11. $\alpha h\nu = (h\nu - E_g)^{1/2}$ where, α is the optical absorption coefficient, $h\nu$ is the photon energy, E_g is the direct band gap, and A is a constant. The bandgap energy was observed to be decreased with the increasing annealing temperature due to quantum confinement. The results support our structural analysis discussed in section 3.2.

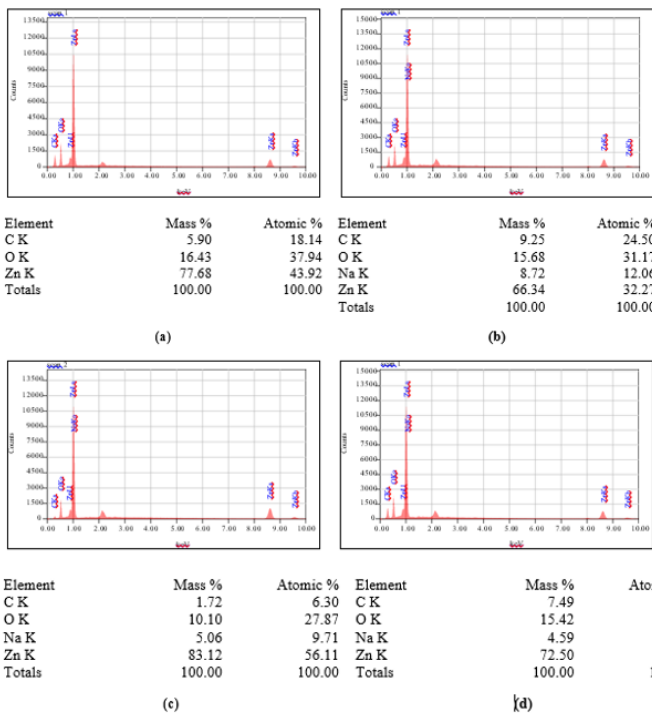


Figure 17: EDX spectrum, and the qualitative analysis of the samples grown at (a) 30°C, (b) 40°C, (c) 50°C, and (d) 60°C.

Whereas the bandgap was increased with the increase in calcination temperature. The peak wavelengths, absorption coefficients, and the bandgaps are plotted in Figure 12 and Figure 13 and listed in Table 4 and Table 5, for the annealing and calcination temperatures respectively. These results indicate that the band gap energy can be tuned by varying the annealing and/or calcination temperature for different applications.

Morphology and Composition

The morphological studies of synthesized nanoparticles were carried out by scanning electron microscopy (SEM). (Figures 14-16) represent SEM images of the three sets of ZnO nanoparticles samples that are prepared at different growth temperatures, annealing temperatures, and calcination temperatures respectively. In most of the images, it can be seen that the ZnO

samples have spherical nanoparticles with random orientation. However, some of the samples are non-spherical such as in the case of Figure 14 (a) and (e) which look more like nanoflakes instead of spherical particles. Some of the samples such as in the Figure 15(e) and Figure16 (e) few nanotubes can also be seen. Elemental analysis was done by the energy dispersive x-ray spectroscopy (EDX) for the first set of samples which differ in the growth temperature. The EDX spectra of the four samples grown at 30°C, 40°C, 50°C, and 60°C are shown in Figure 17 (a) to (d) respectively. The EDX spectra confirm the existence of zinc (Zn), and O (oxygen), in ZnO matrix. A predominant peak corresponds to Zn. However, significantly small peaks of C in all the four samples, and the peaks Na in the last two samples also appeared which might be due to some of the biproducts.

Table 1: Crystallite size and lattice constant for the samples Grown at different temperatures.

Growth Temperature °C	Crystallite size nm	Lattice constant Å
20	28.76	3.2542
30	29.35	3.2541
40	32.68	3.2544
50	36.31	3.2543
60	38.70	3.2529

Table 2: Crystallite size and lattice constant for the samples Annealed at different temperatures.

Annealing Temperature °C	Crystallite size nm	Lattice constant Å
200	17.41	3.2540
300	17.50	3.2505
400	19.01	3.2661
500	19.67	3.2528
600	23.40	3.2565

Table 3: Crystallite size and lattice constant for the samples Calcined at different temperatures.

Calcination Temperature °C	Crystallite size nm	Lattice constant Å
450	26.55	3.2559
500	26.84	3.2571
550	26.33	3.2554
600	25.26	3.2534

Results and Discussions

The XRD patterns of the synthesized nanoparticles are shown in (Figures 2-4) which show that the particles are of hexagonal wurtzite structure. As discussed in section-3.1 the crystallite sizes are observed to be varied for varying temperatures at the time of growth, annealing, and calcination. The crystallite sizes are observed to range from 28.76nm to 38.70nm, 17.41nm to 23.40, and 26.84nm to 25.25nm for temperatures ranging from 20°C to 60°C growth temperatures, 200°C to 600°C annealing temperatures, and 450°C to 650°C calcination temperatures, respectively. It is observed that increasing the growth and annealing temperatures the crystallite size also increases, whereas the increase in calcination temperature leads to the decrease in the crystallite size of the ZnO nanoparticles.

Table 4: Peak wavelengths, absorption coefficients, and the bandgap energy for annealing temperature found from the Figure 8 & Figure 10, and plotted in Figure 12.

Annealing Temperature (oC)	Peak Wavelengths (nm)	Absorption Coefficient (cm-1)	Band Gap Energy (eV)
200	301.52	1.07	3.45
300	304.44	1.96	3.15
400	305.54	3.22	3
500	307.72	4.16	2.75
600	308.75	4.89	2.57

Table 5: Peak wavelengths, absorption coefficients, and the bandgap energy for calcination temperature found from the Figure 9 & Figure 11, and plotted in Figure 13.

Calcination Temperature oC	Peak Wavelengths (nm)	Absorption Coefficient (cm-1)	Band Gap Energy (eV)
450	262.69	2.71	3.94
500	260.85	2.18	4.19
550	260.53	1.98	4.31
600	258.7	1.64	4.5
650	257.66	1.35	4.63

The UV-VIS analysis discussed in section-3.2 shows that the bandgap of the ZnO nanoparticles can be tuned by varying the annealing or calcination temperatures. The bandgap of the ZnO samples annealed at temperatures 200°C to 600°C decreased from 3.45eV to 2.57eV, while in the case of varying calcination temperatures the bandgap increased from 3.94eV to 4.63eV. The morphological studies show that most samples have nanoparticles that are of spherical shape, while nanoflakes and nanotubes were also seen in few samples. The elemental studies were also done using the EDX analysis technique, and the results can be seen in Figure 17 above.

Conclusion

The Zinc Oxide (ZnO) nanoparticles were successfully synthesized by the solgel method, which is a time taking, but a low-cost synthesis technique. Obtained nanoparticles were successfully analyzed for structural, optical, morphological, and compositional studies. The dependencies of the crystallite size and the bandgap of the ZnO particles on the growth temperature, annealing temperature, and calcination temperature were successfully studied. The comparison of the above-said cases is successfully presented.

Acknowledgment

We are heartily thankful to our mentor, Dr. Shahid Mahmood, Professor, Department of Physics, University of Karachi, who provided us the opportunity to work at his great Spectroscopy research laboratory where we performed most of the work in a peaceful and calm environment.

References

- Filip MR, Eperon GE, Snaith HJ, Giustino F. Steric engineering of metal-halide perovskites with tunable optical band gaps. *Nature communications*. 2014; 5: 5757.
- Zhang P, Liu Z, Duan W, Liu F, Wu J. Topological and electronic transitions in a Sb (111) nanofilm: The interplay between quantum confinement and surface effect. *Physical Review B*. 2012; 85: 201410.
- Tavakoli S, Kharaziha M, Nemati S. Polydopamine coated ZnO rod-shaped nanoparticles with noticeable biocompatibility, hemostatic and antibacterial activity. *Nano-Structures Nano-Objects*. 2021; 25: 100639.
- Sun S, Murray CB, Weller D, Folks L, Moser A. Monodisperse FePt nanoparticles and ferromagnetic FePt nanocrystal superlattices. *Science*. 2000; 287: 1989-1992.
- Hisatomi T, Kubota J, Domen K. Recent advances in semiconductors for photocatalytic and photoelectrochemical water splitting. *Chemical Society Reviews*. 2014; 43: 7520-7535.
- Umar A, Kumar R, Kumar G, Algarni H, Kim SH. Effect of annealing temperature on the properties and photocatalytic efficiencies of ZnO nanoparticles. *J Alloys Compounds*. 2015; 648: 46-52.
- Yang J, Liu X, Yang L, Wang Y, Zhang Y, Lang J, Gao M, Feng B. Effect of annealing temperature on the structure and optical properties of ZnO nanoparticles. *J Alloys Compounds*. 2009; 477: 632-635.
- Ali D, Muneer I, Butt MZ. Influence of aluminum precursor nature on the properties of AZO thin films and its potential application as oxygen sensor. *Optical Materials*. 2021; 120: 111406.
- Gao Y, Hai P, Liu L, Yin J, Gan Z, et al. Balanced crystallinity and nanostructure for SnS2 nanosheets through optimized calcination temperature toward enhanced pseudocapacitive Na+ storage. *ACS Nano*. 2022; 16: 14745-14753.



10. Carp O, Huisman CL, Reller A. Photoinduced reactivity of titanium dioxide. *Progress in solid state chemistry*. 2004; 32: 33-177.
11. Jaafar SH, Zaid MH, Matori KA, Aziz SH, Mohamed Kamari H, Honda S, Iwamoto Y. Influence of Calcination Temperature on Crystal Growth and Optical Characteristics of Eu³⁺ Doped ZnO/Zn₂SiO₄ Composites Fabricated via Simple Thermal Treatment Method. *Crystals*. 2021; 11: 115.